COPY NO.

IMM-NYU 231
JUNE 1956

NEW YORK UNIVERSITY
INSTITUTE OF
MATHEMATICAL SCIENCES

Instability of Liquid Surfaces and the Formation of Drops.

Part II: — A Refined Theory

by IGNACE I. KOLODNER

PREPARED UNDER
CONTRACT NO. DA-18-064-404-CML-28
CHEMICAL CORPS, U. S. ARMY

IMM-NYU 231
June 1956

Instability of Liquid Surfaces and the Formation of Drops. Part II – A Refined Theory

by

Ignace I. Kolodner

This report represents results obtained at the Institute of Mathematical Sciences, New York University, under the sponsorship of the United States Army Chemical Corps, Contract No. DA-18-064-404-CML-28.

I. Introduction

In an earlier paper [2] we showed how the notion of Taylor instability can be used to explain the break-up of accelerated thin liquid sheets into drops, and how on the basis of this theory the drop sizes can be estimated. The idea underlying the calculation is as follows: One considers a plane layer accelerated in a direction normal to its surface by imposing, e.g., a pressure difference on opposite surfaces. The zero order motion — which incidentally is an exact solution for the plane layer — is a parallel flow with the velocity of bounding surfaces. It is next argued that the flow actually deviates from the zero order solution because either the bounding surfaces are not perfectly plane, or the pressure on the boundary is not exactly constant, or because of some random perturbation that may occur at the outset or during the motion. To see what happens to the bounding surfaces, one considers the first order perturbation which satisfies linear equations and is represented by a series (or integral) of normal modes. Some of these modes are found to be unstable in the sense that their amplitudes grow unrestrictedly with time. Among these one or more may be called <u>most unstable</u> in the sense that they grow most rapidly. When the acceleration of the layer is constant the unstable modes grow exponentially and the most unstable modes have the largest exponent. The most unstable modes are assumed responsible for break-up of the sheet by <u>pinching</u> it into pieces which eventually become spherical drops under

the influence of surface tension.

On the basis of the above mechanism one gets an estimate of the number of drops produced per unit area and subsequently a formula for their radii. This formula is

$$r = \left(\frac{9\pi T h^2}{2(p_1 - p_2)}\right)^{1/3} \tag{1}$$

where

h — thickness of the sheet

T — coefficient of surface tension

$(p_1 - p_2)$ — difference of pressures exerted on different sides of the layer.

The formula (1) was obtained under the assumption that the liquid is incompressible and inviscid. As it indicates, the notion of surface tension plays a basic role. Without it, indeed, the notion of maximum instability would not exist. Concerning this see also [1].

A formula such as ( ) is of considerable practical importance, yet its validity is in doubt. Even if one does not question the correctness of the mechanism used to explain the process of dropletization, a doubt arises from an unqualified extrapolation of the notion of instability by means of which the formula has been obtained. Although the existence of instabilities is unquestionable, it is not at all certain that small disturbances will grow sufficiently to produce pinching as the linearized perturbation theory indicates. That an indiscriminate growth of perturbations may be arrested is indicated by the experiments of Lewis [5]. Since then, Layzer [4] has shown by means of a more

refined theoretical considerations that the growth of unstable modes is indeed arrested. The calculations by Pennington and others [6] point to the same. Layzer's and Pennington's papers deal with the Taylor case — half infinite liquid medium without consideration of effects of surface tensions — and their result is thus much more striking.

Nevertheless, accelerated sheets do desintegrate. The outstanding question is then whether the mechanism of desintegration proposed in [2] is justifiable; and whether the formula (1) has at least a limited practical value. In [2] a precaution is taken by stating that the treatment applies to thin sheets. What is needed is a qualification of what this means in this problem and a description of what happens when the sheet is not thin. In this paper we shall present a partial answer to these questions.

While formula (1) predicts a natural desintegration of sheets into drops of definite size, a question arises about what happens to an accelerated sheet when initially one surface of the layer is deformed in a controlled way, by introducing, e.g., slight dimples distributed periodically. This poses an initial value free boundary problem, which is, of course, very difficult to handle. We consider here a very special problem of this type, namely that in which one surface is kept rigid, while the other surface has a sinusoidal profile. That is, the profile is given initially

by the equation

$$(2) \qquad z = a \cos \frac{x}{\lambda} .$$

We can treat also the case when the equation of the surface is initially

$$(3) \qquad z = a \cos \frac{x}{\ell} \cos \frac{y}{\ell} ,$$

but this would lead to technical complications without adding to the understanding of the behavior of the layer.

It turns out that the equation for the surface at any time can be expressed as a formal power series in a/l which probably has an asymptotic character. Furthermore, with the assumed initial data (2) (or (3), which we do not consider here), and in these cases only, this series can be computed to any order. We carried our considerations up to terms of third order, and to this order our results seem to agree with other theoretical considerations and with some experimental results. (It is not known whether the consideration of higher approximations would improve the accuracy of these results.)

In Section 2 the mathematical problem is formulated. In Section 3 we consider the instability theory, i.e. the first order approximation as applied to the case of surfaces having one dimensional profile. In Section 4 we present the method of solution which is followed in Section 5 with explicit results up to terms of third order. Section 6 contains a discussion of these results.

We consider sheets both of finite and infinite thickness. As to the latter, our results agree satisfactorily with those of Pennington [5] who used a high speed electronic computer to study the growth of instability. They also show an arrest of instabilities as predicted in [5] and [6].

Concerning sheets of finite thickness, our study of their time history shows at first an amplification of their initial deformation followed in many cases by the formation of jets at the trough of the layer, see Figures 8, 10, and 12. This feature is very plausible, as can be seen from the following qualitative description of the layer based on the assumption of incomprensibility of the liquid, see Fig. 1-a, -b,-c, page 6.

Figure 1a shows the initial configuration. The liquid is at rest but the lower surface is deformed. The upper surface will be kept plane during the motion. As the layer is accelerated upwards, the deformations of the lower (free) surface will grow, due to instability. At least during an early stage of the motion, liquid will flow generally away from the troughs into the crests of the surface. This is indicated in Fig. 1b by arrows along the streamlines. As the motion progresses, either the sheet will break or the growth of the instabilities will be arrested. The first possibility is exactly the basis for the theory of break-up proposed in [2]. In the other case there will be a time at which the velocities in the fluid will reverse their direction. At that time due to high velocities at the troughs of the

$t = t_o$

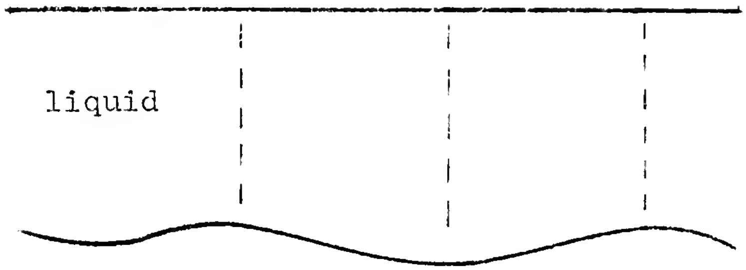

Fig. 1a

$t = t_1 > t_o$

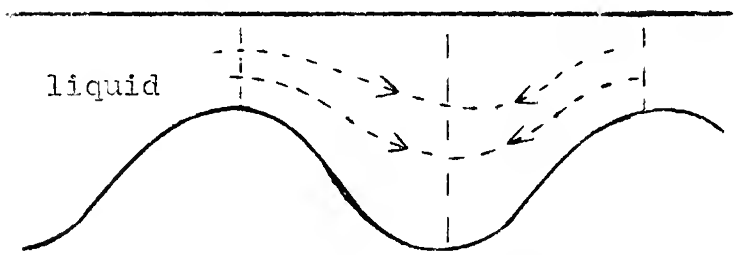

Fig. 1b

$t = t_2 > t_1$

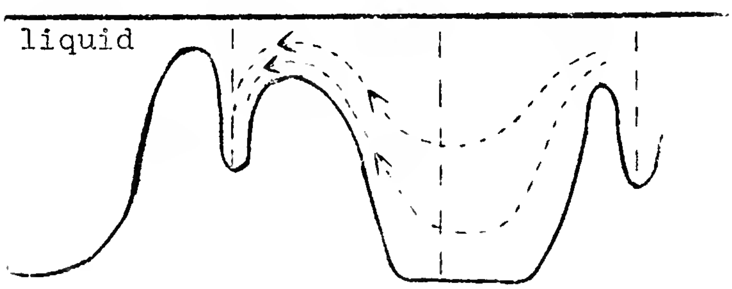

Fig. 1c

direction of acceleration

layer, jets will be produced as indicated in Fig. 1c. A similar situation was observed experimentally by T. Holland(1) who used high speed photography to study the early history of accelerated sheets.

As to the later history of the sheet, our results seem to confirm to a certain degree those of the instability theory. As time progresses the deformation becomes so large that the sheet breaks into filaments by pinching. If one starts with a deformation whose wavelength is approximately equal to the critical wavelength given by the instability theory, the breakdown is into approximately one filament per wavelength. If it is twice the critical wavelength, the breakdown is into two filaments, which are not, however, of same size. If finally, it is three times the critical wavelength, the breakdown is into three filaments. This is in particular true when the sheet thickness is less than the critical wave length. For thick sheets our theory may not be adequate. In all cases our result shows a slower rate of deformation than that predicted by the instability theory.

Although we have treated only the case of a one dimensional profile, which leads to a break of sheets into filaments, our results indicate that they apply equally well to the two dimensional profile, when a desintegration into drops is expected. Our conclusion is thus that the formula (1) is adequate for the case when the sheet thickness is small compared to the critical wavelength.

---

(1) Oral communication. The author is indebted to Dr. T. Holland for making these results available.

2. Formulation of the free boundary problem.

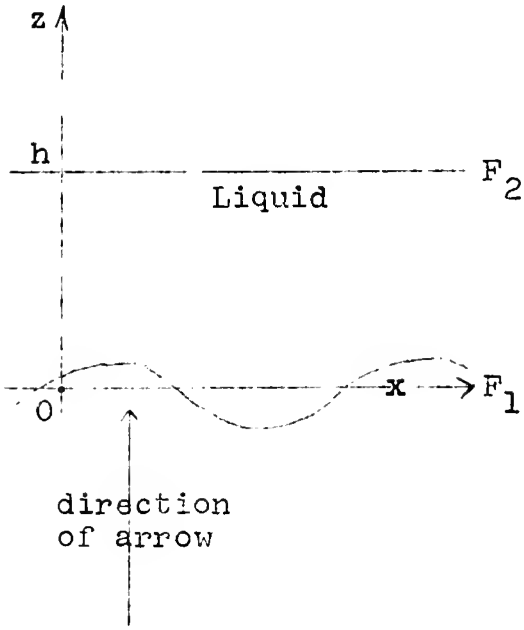

Fig. 2

Consider a layer of incompressible, inviscid liquid contained between the surfaces F_1 and F_2. Assume that the layer is accelerated upwards with the constant acceleration $a > 0$. The upper boundary is kept plane, while on the lower, free boundary, there is exerted a fixed pressure p augmented by pressure due to surface tension. The equations of the boundaries are

(2.1) $$z = h + \tfrac{1}{2}at^2 \text{ — upper boundary } F_2$$

(2.2) $$z = \tfrac{1}{2}at^2 + Z(x,y,t) \text{ — lower boundary } F_1 ,$$

where h is the average thickness of the layer.
The object is to find $Z(x,y,t)$ for all t given Z, Z_t at $t = 0$.

In the liquid, the velocity field is derived from a potential ϕ satisfying Laplace's equation,

(2.3) $$\Delta \phi = 0.$$

The kinematic boundary conditions are

(2.4) $$\phi_z = at \quad \text{on } F_2 ,$$

(2.5) $$\phi_z - Z_x\phi_x - Z_y\phi_y = at + Z_t \quad \text{on } F_1 .$$

On the free boundary we have furthermore the dynamic condition

stating continuity of pressure,

$$\rho(\phi_t+\tfrac{1}{2}(\nabla\phi)^2 + p + 2TH = f(t), \quad \text{on } F_1 \,. \tag{2.6}$$

Here T is the coefficient of surface tension and $f(t)$ is an arbitrary function of time whose choice is determined by the normalization of the potential ϕ. H is the mean curvature of the free surface given by

$$H = \tfrac{1}{2}((1+Z_y^2)Z_{xx}-2Z_xZ_yZ_{xy}+(1+Z_x^2)Z_{yy})(1+Z_x^2+Z_y^2)^{-\frac{3}{2}} \tag{2.7}$$

We restrict the study to the special case when

$$Z(x,y,o) = x \cos \frac{x}{\ell} \,, \quad Z_t(x,y,o) = 0 \,. \tag{2.8}$$

Since y does not appear explicitly in any of the above equations, the solution will be independent of y. H will, in particular, take on the simpler form

$$H = \tfrac{1}{2}(1+Z_x^2)^{-\frac{3}{2}} Z_{xx} \,. \tag{2.7'}$$

It is convenient to consider the problem in a frame moving with the upper surface, and to introduce dimensionless variables. Chose ℓ and $T = \sqrt{\ell/a}$ for units of length and time respectively. Let

$$
\begin{aligned}
& x = \ell\bar{x},\ y = \ell\bar{y},\ z = \ell\bar{z} + \tfrac{1}{2}a\tau^2\bar{t}^2,\ t = \bar{t} \\
(2.9)\quad & \phi = \frac{\ell^2}{\tau}\bar{\phi}(\bar{x},\bar{y},\bar{z},\bar{t}) + \ell\tau a\bar{t}z + F(t) \\
& Z = \ell\bar{Z}(\bar{x},\bar{y},\bar{t}).
\end{aligned}
$$

The conditions (4),(5), and (6) become, on dropping all bars and setting for convenience

$$F'(t) = \tfrac{1}{2}a^2\tau^2\bar{t}^2 - \frac{p}{\rho} + \frac{1}{\rho}f(\tau\bar{t}) \,,$$

(2.4') $\quad \phi_z = 0, \text{ for } z = \nu \quad ,$

(2.5') $\quad \phi_z = Z_x\phi_x - Z_y\phi_y = Z_t \ , \text{ for } z = Z \quad ,$

(2.6') $\quad \phi_t + \frac{1}{2}(\nabla\phi)^2 + z + 2kH = 0, \text{ for } z = Z \ ,$

where

(2.10) $$\begin{cases} \nu = \dfrac{h}{\ell} \\ k = \dfrac{T}{\rho a \ell^2} \end{cases}$$

Equations (2.3) and (2.7) (2.7') remain unchanged.

The special initial conditions (2.8) become

(2.8') $\quad Z(x,y,0) = \varepsilon \cos x, \ Z_t(x,y,0) = 0 \text{ where } \varepsilon = \frac{a}{\ell}$

The problem contains three parameters. ν is the thickness parameter measured in units of the wave length of the initial disturbance, ε is the amplitude of disturbance, and k may be conveniently called the instability parameter.

3. Instability theory

If we disregard the initial conditions (2.8'), $\phi \equiv 0$, $Z \equiv 0$ give a possible motion of the layer - the so-called zero order motion. The instability theory studies the possible deviations from the zero order solution under the assumption that these deviations are so small that all equations may be justifiably linearized. Assume that

(3.1) $$\begin{cases} \phi = \sum\limits_{\lambda} g(t) \cosh \lambda(\nu - z)\psi_\lambda(x,y) \quad , \\ Z = \sum\limits_{\lambda} f_\lambda(t) \ \psi_\lambda(x,y) \quad , \end{cases}$$

where λ is some indexing system. Equation (2.4') is satisfied

and (2.3) will be satisfied if ψ_λ is a solution of

(3.2) $$\psi_{xx} + \psi_{yy} + \lambda^2\psi = 0 .$$

The remaining two boundary conditions now imply, on linearization that

(3.3) $$-\lambda g \sinh \lambda\nu = \dot{f} ,$$

(3.4) $$\dot{g} \cosh \lambda\nu + (1-k\lambda^2)f = 0$$

Solving for f, one gets

$$f(t) = f_{o1}e^{\alpha t} + f_{o2}e^{-\alpha t}$$

where

$$\alpha^2 = \lambda \tanh \lambda\nu(1-k\lambda^2) .$$

When $\lambda^2 < k^{-1}$, α will be real and therefore the time factors corresponding to those values of λ will grow exponentially. The most unstable mode will correspond to that value of λ_m which maximizes α, i.e. for which $\frac{d}{d\lambda}(\alpha^2) = 0$. λ_m is the solution of

(3.6) $$(1-3k\lambda^2) \text{ th } \lambda\nu + \nu\lambda(1-k\lambda^2)(1-\text{th}^2\lambda\nu) = 0.$$

When $\lambda_m\nu$ is large, we have approximately

(3.7) $$\lambda_m \sim \sqrt{\frac{1}{3k}} .$$

Set

(3.8) $$\lambda_m = \mu\sqrt{\frac{1}{3k}} .$$

Substituting in (6), one gets, after some transformations

(3.9) $$\mu^2 = \frac{\sigma + \sinh \sigma}{\frac{1}{3}\sigma + \sinh \sigma}$$

where $$\sigma = \frac{2\nu\mu}{\sqrt{3k}} .$$

Clearly then $1 < \mu < \sqrt{\frac{3}{2}}$, so that

(3.10) $$\frac{1}{\sqrt{3k}} < \lambda_m < \frac{1}{\sqrt{2k}}$$

For $\nu = \infty$ (Taylor case), $\mu = 1$. Likewise, for $k = 0$ (i.e. when $T = 0$), $\mu = 1$. (In the latter case the notion of maximum instability does not exist.) The table below gives the correction factors μ for those values of ν and k which are used for illustrative purposes in further discussion, Section 6.

Table (3.1)

k	$\lambda_m \sim \sqrt{\frac{1}{3k}}$	μ	
		$\nu = 1$	$\nu = .2$
0	∞	1	1
1/27	3	1.003	1.177
1/12	2	1.045	1.203
1/3	1	1.12	1.219
2/3	.71	1.16	1.222
1	.58	1.18	1.223
∞	0	$\sqrt{\frac{3}{2}}$	$\sqrt{\frac{3}{2}}$

Assume now that the lower surface is a cylinder with generators parallel to y axis. The profile of the surface is then one dimensional, and the liquid flow - two dimensional. From the equation (2) we get, assuming the normalization $\psi(o) = 1$, $\psi'(o) = 0$,

(3.11) $$\psi_\lambda = \cos \lambda x$$

According to the instability theory, the sheet will break into filaments, of width $\frac{2\pi}{\lambda_m}$, that is, into λ_m filaments per section of width 2π.

4. Method of Solution.

We now turn back to the free boundary problem formulated in Section 2. Assume that Z and ϕ can be expanded in formal power series (convergent or asymptotic) in ε and that furthermore the coefficients in these expansions are themselves expanded in Fourier series in x, with period 2π. Thus, quite generally,

$$(4.1) \qquad Z(x,t) = \sum_{n=0}^{\infty} \varepsilon^n \sum_{m=0}^{\infty} (a_{nm}(t) \cos mx + \bar{a}_{nm}(t) \sin mx)$$

$$(4.2) \qquad \phi(x,z,t) = \sum_{m=0}^{\infty} \varepsilon^n \sum_{m=0}^{\infty} (b_{nm}(t) \cos mx + \bar{b}_{nm}(t) \sin mx) \cosh m(\nu - z).$$

Each term in (4.2) satisfies already the conditions (2.3, 2.4'). The problem thus is reduced to the determination of the a's and b's in such a way that the remaining boundary conditions (2.5', 2.6') be also satisfied. The initial conditions (2.8') imply that at t = 0:

$$(4.3) \qquad a_{nm} = \bar{a}_{nm} = \dot{a}_{nm} = \dot{\bar{a}}_{nm} = 0, \text{ for all n and m except that}$$

$$(4.4) \qquad a_{11} = 1 .$$

To determine the a's and b's, we substitute (4.1) and (4.2) in (2.5', 2.6'), carry out the intended operations, group terms of like powers of ε, and lastly expand each coefficient in a Fourier series in x. This results in each case in an equation of the form

$$(4.5) \qquad \sum_{n=o}^{\infty} \varepsilon^n \sum_{m=\cdot}^{\infty} (X_{nm} \cos mx + \bar{X}_{nm} \sin mx) \equiv 0 ,$$

where the X's depend on the a's and b's only. Equation (4.5) implies that all the X's are identically zero, thus leading to an infinite set of equations for the a's and b's.

On setting $\varepsilon = 0$, one gets the case when the initial free surface is undeformed. In that case the solution is the zero order solution,

$$Z \equiv 0, \ \phi \equiv 0 \ ;$$

hence

$$a_{om} \equiv \bar{a}_{om} \equiv b_{om} \equiv \bar{b}_{om} \equiv 0 \ . \tag{4.6}$$

With an arbitrary initial Z there would be for every $n \geq 1$ an infinite number of equations to solve. Thus in general we would not be able to obtain any results beyond the terms of first order in ε. The choice of the particular initial Z given by equation (2.8') is motivated by the fact that in this case (and in this case only) for each value of the first index there is only a finite number of not identically vanishing a's and b's; furthermore, the equations for these can be solved in succession. More precisely the following is true:

1. $\bar{a}_{nm} = \bar{b}_{nm} \equiv 0$, for all m and n.
2. $a_{no} = 0$, for all n
3. The pairs (a_{nm}, b_{nm}) satisfy equations of the form

$$\begin{cases} \dot{a}_{nm} + (m \sinh m\nu) b_{nm} = f_{nm}, \\ (\cosh m\nu)\dot{b}_{nm} + (1-km^2) a_{nm} = g_{nm} \ , \end{cases} \tag{4.7}$$

where f_{nm} and g_{nm} are polynomials in $a_{k\ell}$, $\dot{a}_{k\ell}$, $b_{k\ell}$, $\dot{b}_{k\ell}$,

with $k < n$, and of weight n with respect to the first index, and furthermore, $f_{nm} \equiv g_{nm} \equiv 0$ whenever:

$$m > n \quad \text{for any } n,$$

$$\text{or} \qquad n+m = \text{odd integer, any } n \text{ and } m.$$

From (4.7) we obtain

$$(4.8) \qquad \ddot{a}_{nm} - \alpha_m^2 a_{nm} = f_{nm} - (m \operatorname{th} m\nu) g_{nm} \; , \quad \alpha_m^2 = m(1-km^2) \operatorname{th} m\nu \; ,$$

and

$$(4.9) \qquad b_{nm} = \frac{f_{nm} - \dot{a}_{nm}}{m \sinh m\nu} \, .$$

Since the equations (4.8) are homogeneous for values of m and n listed above, and since the initial data for the a's are also homogeneous for these values, one gets from (4.8) and (4.9),

$$(4.10) \quad a_{nm} \equiv b_{nm} \equiv 0 \quad \text{for } m > n, \text{ or when } n+m = \text{odd integer.}$$

The third part of the theorem implies then that the coefficients of ε^n in (4.1) and (4.2) are terminating series with at most $[\frac{n}{2}]+1$ non-indentically vanishing terms.

Part 1 of the theorem is proven by demonstrating that both Z and ϕ must be even functions of x.(2) Part 2 is shown by observing that incompressibility and periodicity of the

---

(2) It is not true however that $Z(x,t)$ would be an odd function of x if $Z(x,o)$ were odd. Consider, for example, the same problem and set $x=(\xi-\frac{\pi}{2})$. Using ξ as an independent variable we would be faced with exactly the same problem with ξ replacing x throughout and with the initial data $\bar{Z}(\xi,o) = Z(x,t) = \varepsilon \sin \xi$ replacing (2.8'). The solution for $\bar{Z}$ is

$$\bar{Z}(\xi,t) = Z(x,t) = \sum_{n=o}^{\infty} \varepsilon^n \sum_{m=o}^{k} \frac{1}{2} a_{nm}(t) \left[(i^m + i^{-m}) \cos m\xi - i(i^m - i^{-m}) \sin m\xi \right]$$

which is odd in ξ.

problem imply the conservation of volume in a wave length. Hence

$$V(t) = \int_0^{2\pi} (\nu - ?(x,t))dx = \text{constant} = 2\pi(\nu - \sum_{n=0}^{\infty} a_{no}\varepsilon^n) \equiv 2\pi\nu.$$

Consequently, $a_{no} \equiv 0$ for all n. Proof of part 3 preceeds by induction on n and is rather involved. Since it is similar to that given in an analogous case in [3], Appendix, we omit it here.

In view of the theorem only the following coefficients are not identically zero:

a_{11} , b_{11}

a_{22} , b_{20} , b_{22}

a_{31} , a_{33} , b_{31} , b_{33} etc.

As one goes further, the number of coefficients to be computed increses and also the equations that determine them become more complicated. While the work involved is straight forward, the amount of work in, say, fourth approximation is already prohibitive. It is, however, possible to characterize the results further without an explicit determination, with which we now proceed.

It turns out that $f_{11} \equiv 0$, $g_{11} \equiv 0$. Consequently, from equation (4.8), $a_{11} = \cosh \alpha_1 t$. We use here the notation

$$\alpha_m = +\sqrt{|\alpha_m^2|} \ , \ \alpha_{-m} = -\sqrt{\alpha_m^2} \ , \ \text{if } \alpha_m^2 > 0$$

$$\alpha_m = +i\sqrt{|\alpha_m^2|} \ , \ \alpha_{-m} = -i\sqrt{|\alpha_m^2|} \ , \ \text{if } \alpha_m^2 < 0.$$

It now can be shown by induction on n that a_{nm} is made of terms of the form

$$P_n(t)e^{\alpha t} .$$

Here:

P_n - is a polynomial of order not exceeding n

$$\alpha = \sum_i \alpha_{m_i} , \quad \text{with} \sum_i |m_i| \leq n .$$

In particular, when all the $m_i > 0$, and $\sum m_i = n$, one shows that $P_n(t)$ is a constant. This information now suffices to determine the behavior of a_{nm} for large t. We distinguish two cases:

Case 1: $k < 1$, i.e. $\alpha_1^2 > 0$

We have,

$$m^2\alpha_1^2 - \alpha_m^2 = m\left[m(1-k)\operatorname{th}\nu-(1-m^2k)\operatorname{th} m\nu\right] \geq m\operatorname{th} m\nu\,(m^2-1)k \geq 0,$$

since $m\operatorname{th}\nu \geq \operatorname{th} m\nu$. Hence

$$|\alpha_m| \leq m\alpha_1$$

and consequently

$$|\alpha| = |\sum \alpha_{m_i}| \leq \alpha_1 \sum |m_i| \leq n\alpha_1$$

Clearly then the dominant term (for t large) in the expression for a_{nm} is of the form

$$\text{constant x } e^{n\alpha_1 t}$$

This certainly implies divergence of the series for $t \to \infty$, showing that either our procedure fails for large t, or that the assumption of a well defined lower surface of the layer is untenable for large t. There is no indication that the series (4.1) and (4.2) converge for any t. The explicit results of the next section actually indicate that at best

an asymptotic behavior of these series may be expected. Thus one would not necessarily improve the accuracy of results by increasing the number of terms under consideration. While we lack a criterion on how many terms it is best to keep for each t, retention of terms up to order ε^3 leads to a description in qualitative agreement with the observed behavior of the layer.

Case 2: $k \geq 1$, i.e. $\alpha_1^2 \leq 0$

Since in this case $\alpha_m^2 \leq 0$ for all m, α is pure imaginary and a_{nm} grows at most as t^n. This case leads to results similar to those that would be obtained if the layer were accelerated in the opposite direction(3). The latter leads to a stable configuration, namely, to standing waves. We may therefore anticipate a similar situation in the case $k \geq 1$, that is, when T is large, or a and λ are small.

Further discussion will be restricted to the case 1 only.

5. Explicit results up to terms in ε^3.

Carrying out the program described in the preceeding section up to terms in ε^3 , one gets the following: From substitution of (4.1,2) in (2.5¹).

---

(3) In that case the formulation of the problem would be essentially the same, except for replacing a by |a| in formula for τ and k, and changing the sign in front of z in equation (2.6'). On using the same formalism, we would get for the α_m the formula

$$\alpha_m^2 = -m(1+km^2)\text{th } m\,\nu \;.$$

Thus all α_m would be pure imaginary.

$$(5.1)\begin{cases} f_{11} = 0 \\ f_{22} = a_{11}b_{11}\cosh\nu \\ f_{31} = a_{11}b_{22}\cosh 2\nu - \frac{1}{2}a_{22}b_{11}\cosh\nu - \frac{1}{8}a_{11}^{2}b_{11}\sinh\nu \\ f_{33} = 3a_{11}b_{22}\cosh 2\nu + \frac{3}{2}a_{22}b_{11}\cosh\nu - \frac{3}{8}a_{11}b_{11}\sinh\nu . \end{cases}$$

From substitution of (4.1,2) in (2.6'),

$$(5.2)\begin{cases} g_{11} = 0 \\ g_{20} = \frac{1}{2}a_{11}b_{11}\sinh\nu - \frac{1}{4}b_{11}^{2}\cosh^{2}\nu - \frac{1}{4}\dot{a}_{11}^{2} \\ g_{22} = \frac{1}{2}a_{11}\dot{b}_{11}\sinh\nu + \frac{1}{4}b_{11}^{2} \\ g_{31} = -\frac{3}{8}ka_{11}^{3} + a_{11}\dot{b}_{22}\sinh 2\nu - \frac{3}{8}a_{11}^{2}\dot{b}_{11}\cosh\nu \\ \qquad + \frac{1}{2}a_{22}\dot{b}_{11}\sinh\nu - b_{11}b_{22}\cosh 3\nu + \frac{1}{2}a_{11}b_{11}^{2}\sinh 2\nu \\ g_{33} = \frac{3}{8}ka_{11}^{3} + a_{11}\dot{b}_{22}\sinh 2\nu - \frac{1}{8}a_{11}^{2}\dot{b}_{11}\cosh\nu \\ \qquad + \frac{1}{2}a_{22}\dot{b}_{11}\sinh\nu + b_{11}b_{22}\cosh\nu . \end{cases}$$

Using (5.1,2) in (4.8) we now get explicit equations for the a_{nm} which can be solved in terms of elementary trancendentals, We get, using the initial conditions (4.3,4),

$$(5.3)\begin{cases} a_{11} = \cosh \alpha_1 t \\ a_{22} = \frac{1-k}{2\alpha_2^2}(\cosh\alpha_2 t - 1) \\ \qquad + \frac{1-k}{2}\left(1+\frac{2}{\cosh 2\nu}\right)(4\alpha_1^2-\alpha_2^2)^{-1}(\cosh\alpha_2 t - \cosh 2\alpha_1 t) \\ a_{31} = A\cosh(\alpha_1+\alpha_2)t + B\cosh(\alpha_2-\alpha_1)t + C\cosh 3\alpha_1 t \\ \qquad + Dt\sinh\alpha_1 t - (A+B+C)\cosh\alpha_1 t \\ a_{33} = \bar{A}\cosh(\alpha_1+\alpha_2)t + \bar{B}\cosh(\alpha_2-\alpha_1)t + \bar{C}\cosh 3\alpha_1 t \\ \qquad + \bar{D}\cos\alpha_1 t - (\bar{A}+\bar{B}+\bar{C}+\bar{D})\cosh\alpha_3 t . \end{cases}$$

$A, B, C, D, \bar{A}, \bar{B}, \bar{C}$, and $\bar{D}$ are numcrical coefficients (depending on the parameters ν and k) which are too cumbersome to be reproduced here. Their exact values, however, were used in the calculations discussed in Section 6.

Simplified approximate expressions for the a_{nm} can be obtained for small t, for large t, and for particular values of ν and k. For t small, we get, using power series expansions in t,

$$(5.4)\quad \left\{\begin{aligned}
a_{11} &\sim 1 + \frac{\alpha_1^2}{2} t^2 \\
a_{22} &\sim -\frac{1-k}{2\cosh 2\nu} t^2 - \frac{(1-k)^2}{12} \operatorname{th}\nu \left(1 + \frac{2}{\cosh 2\nu}\right. \\
&\qquad + \frac{2(1-4k)}{(1-k)(1+\operatorname{th}^2\nu)\cosh 2\nu} t^4 \\
a_{31} &\sim \left[\frac{1-k}{4} \operatorname{th}\nu(\operatorname{th}\nu \operatorname{th} 2\nu - \frac{3}{2}) + \frac{3}{16} k \operatorname{th}\nu\right] t^2 \\
a_{33} &\sim \left[\frac{3}{16}(1-k)(3\operatorname{th}\nu + \operatorname{th} 3\nu - 4\operatorname{th}\nu \operatorname{th} 2\nu \operatorname{th} 3\nu) + \frac{9}{16} k \operatorname{th} 3\nu\right] t^2
\end{aligned}\right.$$

For large t, we get, keeping the dominant terms

$$(5.5)\quad \left\{\begin{aligned}
a_{11} &\sim \frac{1}{2} e^{\alpha_1 t} \\
a_{22} &\sim -\frac{1}{4}(1-k)\left(1 + \frac{2}{\cosh 2\nu}\right)(4\alpha_1^2 - \alpha_2^2)^{-1} e^{2\alpha_1 t} \\
a_{31} &\sim \frac{1}{32} \left[(1-k)(4\alpha_1^2 - \alpha_2^2)^{-1}\left(\frac{\alpha_2^2}{4\alpha_1^2 \sinh 2\nu} - \frac{3}{2} \operatorname{cth} 2\nu\right)\left(1 + \frac{2}{\cosh 2\nu}\right)\right. \\
&\qquad \left. + \frac{3k \operatorname{th}\nu}{16\alpha_1^2} + \frac{\operatorname{th}^2\nu + \operatorname{cth}^2\nu - 6}{8(1+\operatorname{th}^2\nu)}\right] e^{3\alpha_1 t}
\end{aligned}\right.$$

$$(5.5)\left|\begin{aligned} a_{33} \sim \frac{1}{16}\,(9\alpha_1^2-\alpha_3^2)^{-1}\Big\{ & 3(1-k)\left(1+\frac{2}{\cosh 2\nu}\right)(4\alpha_1^2-\alpha_2^2)^{-1}\Big(\alpha_1^2[4\ \mathrm{cth}\ \nu \\ & + \mathrm{th}\ \nu - \mathrm{th}\ 3\nu + \frac{\mathrm{th}\ 3\nu}{2\sinh^2\nu}] + \alpha_2^2\,[\mathrm{cth}\ 2\nu - \mathrm{th}\ 3\nu]\Big) \\ & - \frac{9}{4}\,k\ \mathrm{th}\ 3\nu - \frac{3}{4}\alpha_1^2\Big(5-4\mathrm{th}\ 2\nu\ \mathrm{th}\ 3\nu + \mathrm{th}\ 3\nu\ \mathrm{cth}\ \nu \\ & + \frac{2(3-\mathrm{th}\ \nu\ \mathrm{th}\ 2\nu)}{\sinh^2 \nu}\Big)\Big\}\, e^{3\alpha_1 t} \end{aligned}\right.$$

Our formulae simplify considerably in the case considered by Taylor [7], that is in the case of a sheet of infinite width ($\nu = 0$), neglecting the effects of surface tension ($t = 0$, hence $k = 0$). Then $\alpha_m = \sqrt{m}$, and

$$(5.6)\begin{cases} a_{11} = \cosh t \\ a_{22} = -\frac{1}{4} + \frac{1}{2}\cosh\sqrt{2}t - \frac{1}{4}\cosh 2\,t \\ a_{31} = \frac{1}{4}\cosh\sqrt{2}t - \frac{1}{16}\cosh 3t - \frac{1}{8}\,t\sinh t - \frac{3}{16} \\ a_{33} = -\frac{3}{4}\cosh t\cosh\sqrt{2}t + \frac{3}{32}\cosh 3t + \frac{9}{32}\cosh t + \frac{3}{8}\cosh\sqrt{3}t. \end{cases}$$

To the order considered, the equation for the profile of the boundary is

$$z = Z(x,t) = \varepsilon a_{11}\cos x + \varepsilon^2 a_{22}\cos 2x + \varepsilon^3(a_{31}\cos x + a_{33}\cos 3x)$$

$$= K\,(\cos x - a\cos 2x + b\cos 3x).$$

Here,

$$(5.8)\begin{cases} K = K(t) = \varepsilon a_{11} + \varepsilon^3 a_{31} \\ a = a(t) = -\dfrac{a_{22}\varepsilon^3}{K} \\ b = b(t) = \dfrac{a_{33}\varepsilon^3}{K}. \end{cases}$$

The shape of the profile at any time depends only on the values of a and b and can be followed by studying in the (a,b) plane the locus (a(t), b(t)). Depending on the region where the representative point is located, various shapes are assumed. We distinguish 4 essentially different groups of shapes, described in the table below for half of the wave-length, i.e. for $o \leq x < \pi$, by listing their consecutive minima and maxima. (At $x = o$ or at $x = \pi$, we have always either a minimum or a maximum.) Since all calculations lead to positive values of a, we restrict our considerations to $a \geq o$.

Table

Location of (a,b)	Shape
Region I: $4a^2+(6b-1)^2 \leq 1$ and $-4a+9b+1 \geq 0, b \leq 2/15$	max, min.
Region II: $4a^2+(6b-1)^2 \geq 1$, $-4a+9b+1 \geq 0, b \geq 2/15$	max, min, max, min.
Region III: $-4a \leq 9b+1 \leq 4a$	min, max, min.
Region IV: $4a+9b+1 \leq 0$	min, max, min, max.

See also Figure 3.

In case of sheets of finite thickness ($\nu < \infty$) a break-down will occur at the time when Z(x,t) first reaches the value ν for some x, since at this time the liquid region will become disconnected. At that time the sheet will break by pinching into filaments which normally would soon acquire a circular cross-section because of effects of surface tension. (If initially Z had the form $Z(x,y,o) = a \cos \frac{x}{\lambda} \cos \frac{y}{\lambda}$ the sheet would break into spherical drops.) Depending on the

location of (a,b) at this time, the sheet may break into one, two, or three filaments per wave-length. Thus, if at that time (a,b) is in Region I, the break is into one filament per wave-length; if it is in Region II, - into either one, two, or three filaments,if it is in Region III, - into two filaments; if it is in Region IV - into two, or three filaments. These statements presuppose, of course, that inclusion of terms up to ε^3 only is adequate for the description of the sheet up to the time of breakdown.

5. Discussion of results

A complete discussion of results is very difficult, since the problem contains three independent parameters. We therefore restrict our considerations to special, but significant cases. Firstly we consider the Taylor case, $v = \infty$. Here, we first choose $k = 0$, $\varepsilon = .01$ in order to compare our results with Pennington's machine calculations [6] who used these data. Next we chose $\varepsilon = .5$ and a selection of values of k. To exhibit the behavior of not too thin sheets, we consider the cases $\nu = 1$, $\varepsilon = .5$ and $\nu = .2$, $\varepsilon = .1$, again for a selection of k. Lastly we consider the behavior of very thin sheets, $\nu << 1$ excited spontaneously, $\varepsilon << \nu$.

1. Taylor case: $\nu = \infty$, $k = 0$, $\varepsilon = .01$

The (a,b) locus is shown in figure 4, while the profile shapes are drawn at various times in figure 5. The dotted line is the profile predicted by the linearized theory at $t = 5.1$ ($Z = .75 \cos x$) and shows that the non-linear theory predicts a slowdown of instability. Our results compare well with

those of Pennington. In particular, the appearance of a bulge near the trough at $t = 4.8$ confirms the same feature deduced from inactive computations.

2. <u>Taylor case, $\nu = \infty$, $\varepsilon = .5$, $k = 0.\ \frac{1}{27}.\ \frac{1}{12}$, 1/3, 2/3, 1</u>

(a,b) loci are in figure 4, profile shapes in figure 6.

3. <u>$\nu = 1$, $\varepsilon = .5$, $k = 0.\ \frac{1}{27}, \frac{1}{12}, \frac{1}{3}$, 2/3, 1</u>

According to the instability theory, this sheet will break into one piece (per wavelength) at $t = 3.04$ for $k = .43$, into two pieces at $t = 1.14$ for $k = .1$, and into three pieces at $t = .66$ for $k = .037$. The results of our computations are shown in figures 7 and 8. It is seen that the sheet breaks into one piece for $k = 2/3$, 1, into two pieces for $k = 0$, 1/12, 1/3, and into three pieces for $k = \frac{1}{27} = .037$. For $k = .037$ the breakdown is at $t = 1.96$, or almost 3 times the time predicted by the instability theory. Except for the case $k = 0$, these results are thus roughly in agreement with those predicted by the instability theory, except for time of breakdown.

4. <u>$\nu = .2$, $\varepsilon = .1$, $k = 0, \frac{1}{27}, \frac{1}{12}, \frac{1}{3}, \frac{2}{3}, 1.$</u>

According to the instability theory, this sheet will break into one piece at $t = 13.5$ for $k = .50$, into two pieces at $t = 3.35$ for $k = .13$, into three pieces at $t = 1.26$ for $k = .05$. The results of our computations are shown in figures 9 and 10. It is seen that the sheet breaks into one piece for $k = 2/3, 1$, two pieces for $k = \frac{1}{3}$, and into three pieces for $k = \frac{1}{12}, \frac{1}{27}, 0$.

Again these results are roughly in agreement with those predicted by the instability theory, except for the time of breakdown.

5. Spontaneous disturbances of thin sheets.

Assume that ε is so small that the shape coefficients remain small until t becomes so large that the dominant terms in these coefficients, formulae (5.5), can be used in place of the exact formulae (5.3). Assume furthermore that ν is so small that a power of ν can be neglected when compared to a lower power of ν. It can be shown that formulae (5.4) simplify then to:

$$(6.1)\qquad \begin{cases} a_{11} \sim \frac{1}{2} e^{\alpha_1 t} \\ a_{22} \sim - \frac{1-k}{16k\nu} e^{2\alpha_1 t} \\ a_{31} \sim - \frac{1+3k}{512k\nu^2} e^{3\alpha_1 t} \\ a_{33} \sim \frac{(1-k)(5-13k)}{1024\, k^2\nu^2} e^{3\alpha_1 t} \end{cases}$$

provided that $k = 0$ and $k \neq 1$.

For a, b, and K, formula (5.8), we now get

$$(6.2)\qquad \begin{cases} K = \nu k(1-k)\sigma^2/a \\ a = \frac{\alpha\sigma}{2-\beta^2\sigma^2} \\ b = \frac{\gamma\sigma^2}{2-\beta^2\sigma^2} \end{cases}$$

where

$$(6.3)\qquad \begin{cases} \sigma = \dfrac{\varepsilon e^{a_1 t}}{4k\nu} \\ a = 1-k \\ \beta^2 = \dfrac{1}{8}\, k(1+3k) \\ \gamma = \dfrac{1}{16}(1-k)(5-13k). \end{cases}$$

Accordingly, Z/ν depends only on two parameters, namely k and σ, and this simplifies the discussion.

For a fixed k, the breakdown of the sheet occurs for that value of σ for which $\max\,(Z/\nu)=1$. The maximum of Z occurs either at $x = 0$ and then

$$(6.4)\qquad Z_{max} = K(1-a+b)$$

or at

$$(6.5)\qquad x = \cos^{-1} \frac{a-\sqrt{a^2-3b+9b^2}}{6b}$$

and then

$$(6.6)\qquad Z_{max} = K\left(-\frac{a^3}{27b^2} + \frac{a}{6b}(1+3b)+|b| \left[\left(\frac{a}{6b}\right)^2+ \frac{1}{4} - \frac{1}{12b}\right]^{\frac{3}{2}}\right) .$$

Using equations (5) and (6), one gets the following equations for σ at the time of breakdown:

either

$$(6.7)\qquad k\left[2\sigma-\sigma^2 (1-k)+ \frac{1}{16}\, \sigma^3 (5-20k+7k^2)\right] = 1 ,$$

or

$$(6.8)\qquad -8k\gamma\left(\frac{a}{6\gamma}\right)^3+k\left(\frac{a}{6\gamma}\right)(2+(3\gamma-\beta^2)\sigma^2)+8k\,|\gamma| \left[\left(\frac{a}{6\gamma}\right)^2 - \frac{1}{6\gamma} + \left(\frac{1}{4} + \frac{\beta^2}{12\gamma}\right)\sigma^2\right]^{\frac{3}{2}} = 1,$$

whichever yields a lower value of σ for a given k. It turns out that for $k \geq .737$ equation (6.7) must be used, while for $k = .737$ equation (6.8) must be used. The locus of (a,b) at the time of breakdown is shown in figure 11.

The locus (a,b) can be obtained from the parametric representation, equation (6.2), or from an explicit equation, obtained by eliminating σ, namely

$$\left(\frac{2\beta^2}{\gamma} b\right)^2 - \left(\frac{2\sqrt{2}\beta}{\alpha} a\right)^2 = 1$$

For each value of k this locus consists of a branch of a hyperbola passing through origin. A few of these loci are shown in figure 11. As $k \to 0$, the limiting position of the locus is the parabola $b = \frac{5}{8}a^2$, and as $k \to 1$, the locus shrinks to a point.

Profiles at the time of breakdown are shown in figure 12 for several values of k. For $k \geq .737$ the sheet breaks into one filament per wavelength. For $k \leq .737$ we have two filaments, except that for very small value of $k(k < .5)$ a breakdown into three pieces may occur.

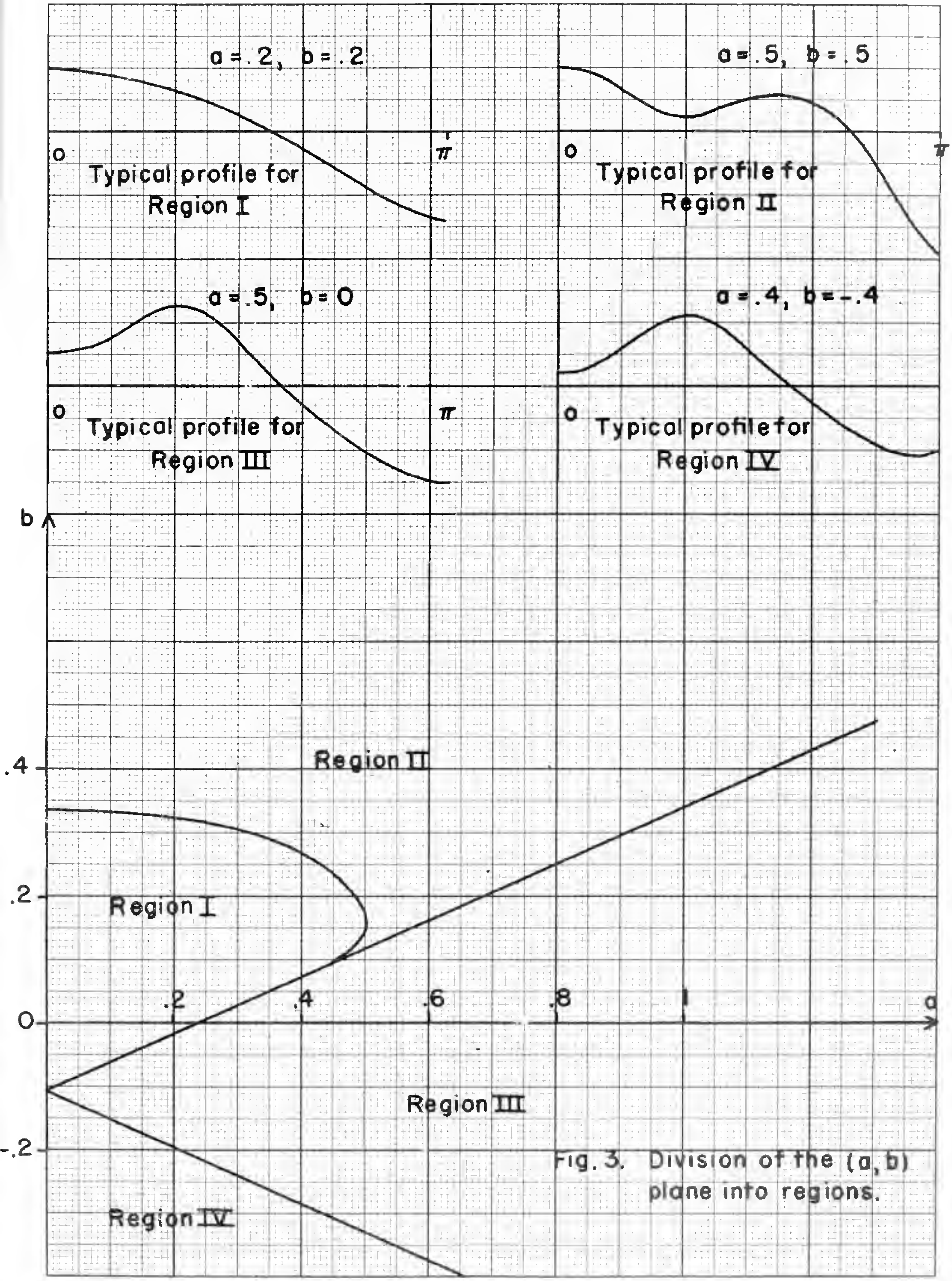

Fig. 3. Division of the (a, b) plane into regions.

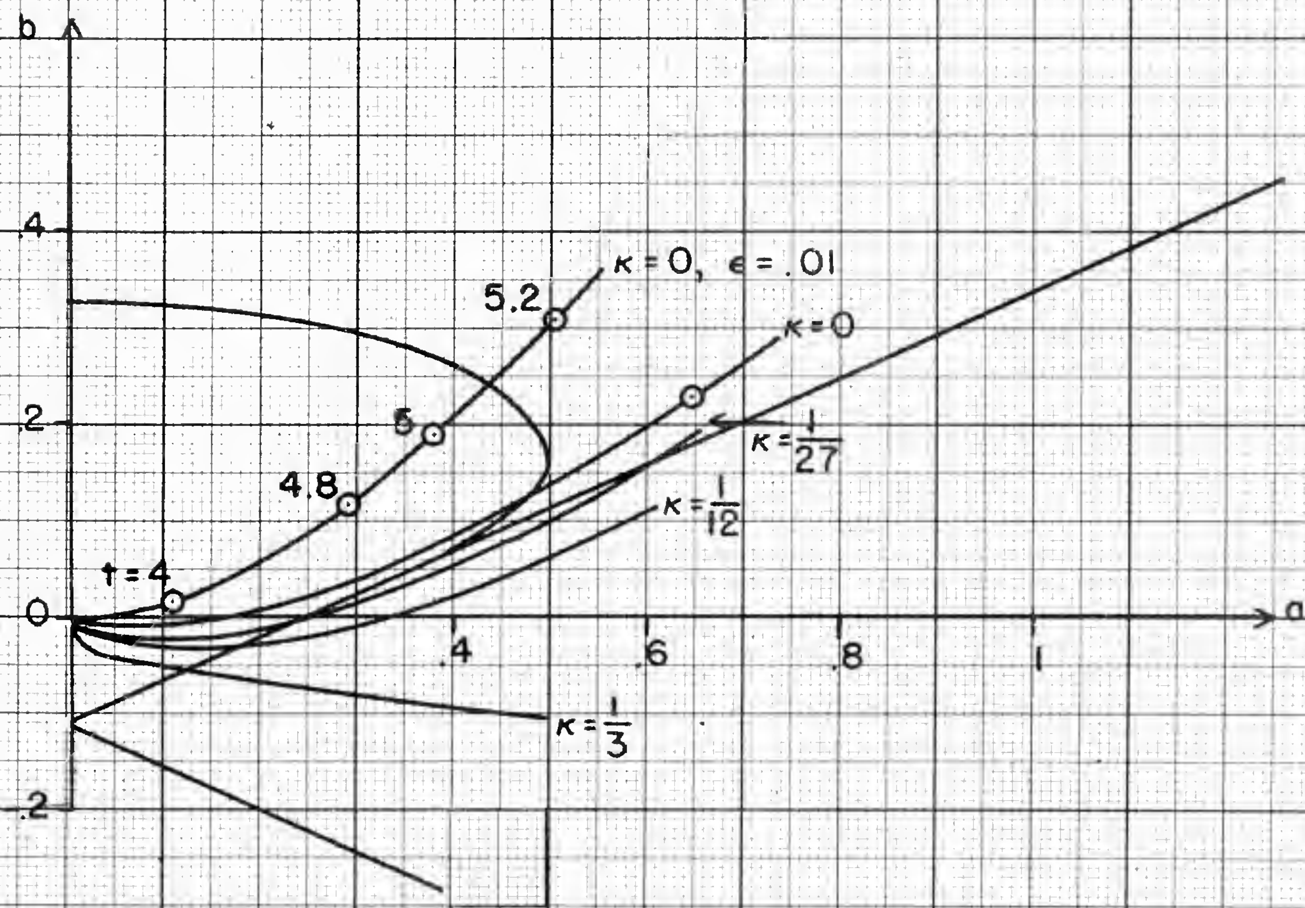

Fig. 4: (a, b) plane diagram for the case $\nu = \infty$, $\epsilon = .5$ (except as noted)

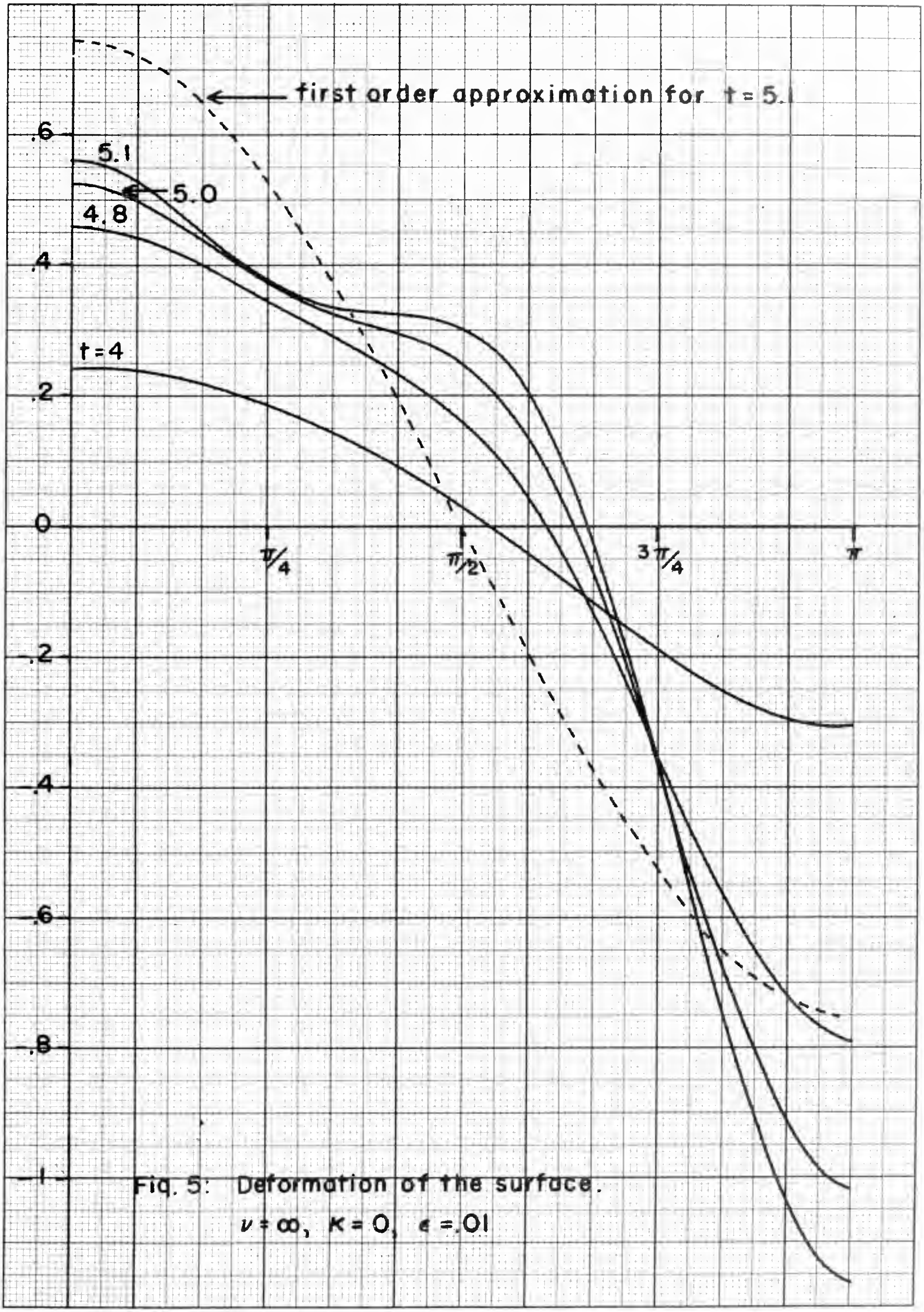

Fig. 5: Deformation of the surface.
$\nu = \infty$, $K = 0$, $\epsilon = .01$

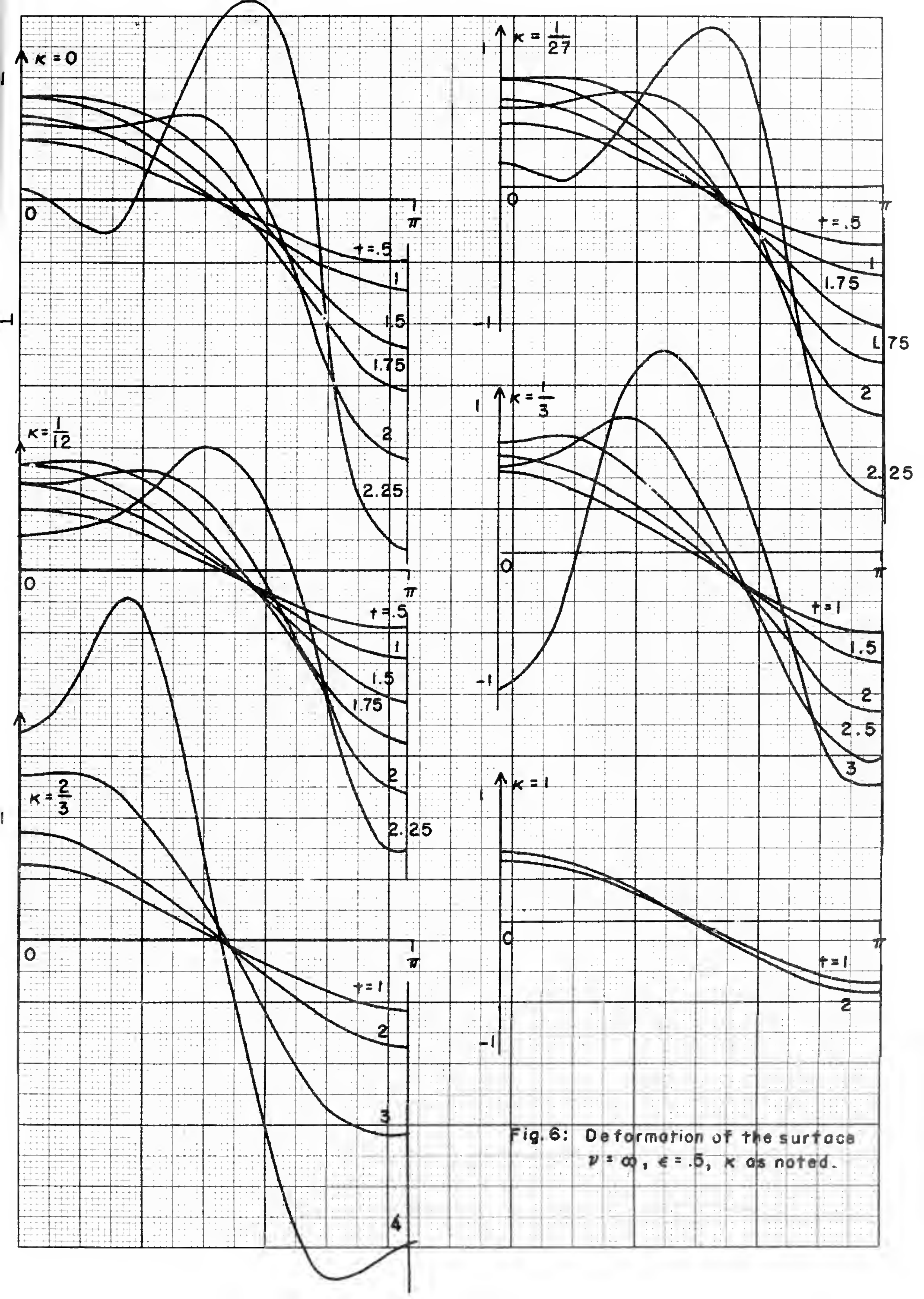

Fig. 6: Deformation of the surface $\nu = \infty$, $\epsilon = .5$, κ as noted.

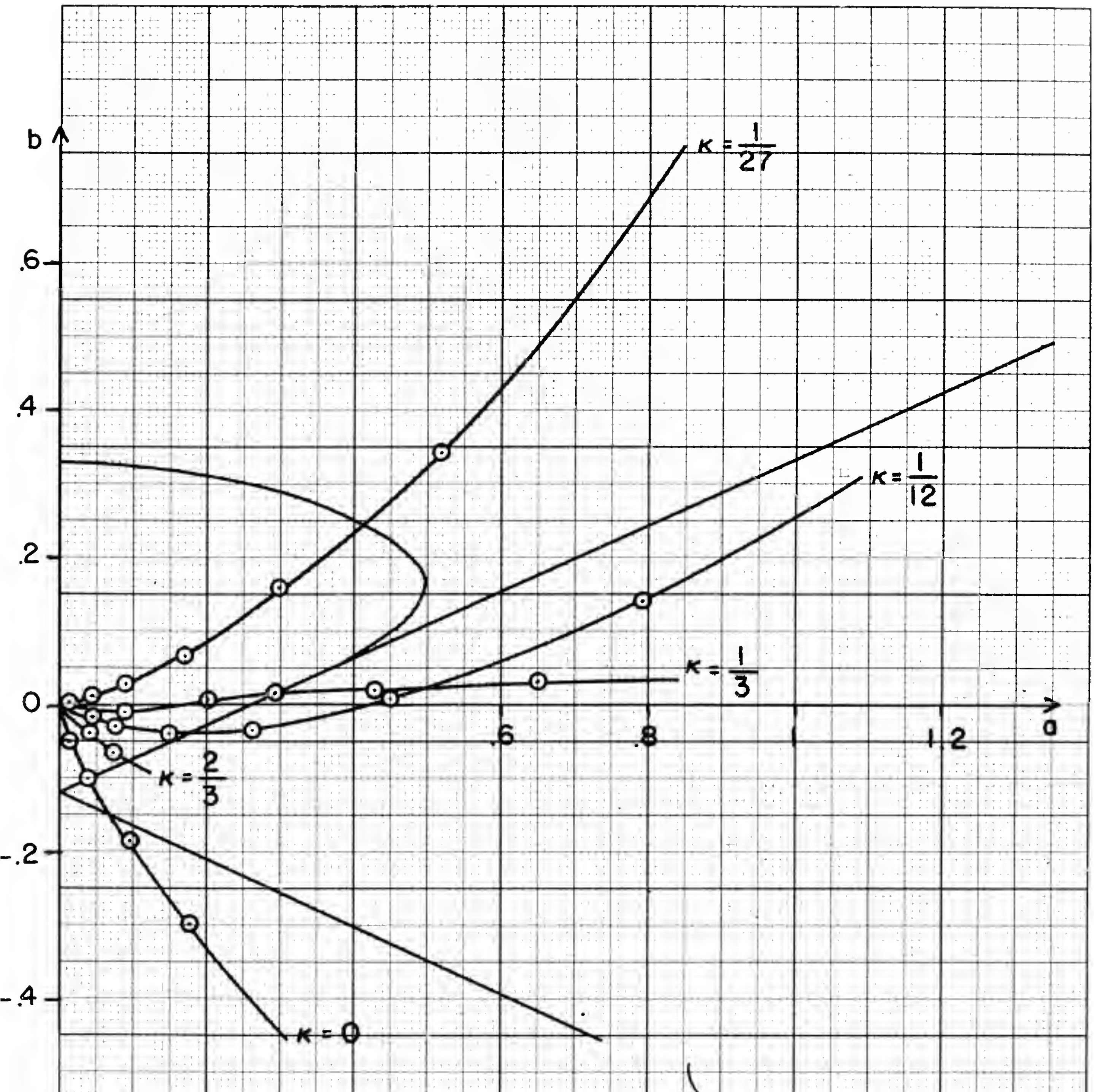

Fig. 7: (a,b) plane diagram for the case $\nu = 1$, $\epsilon = .5$

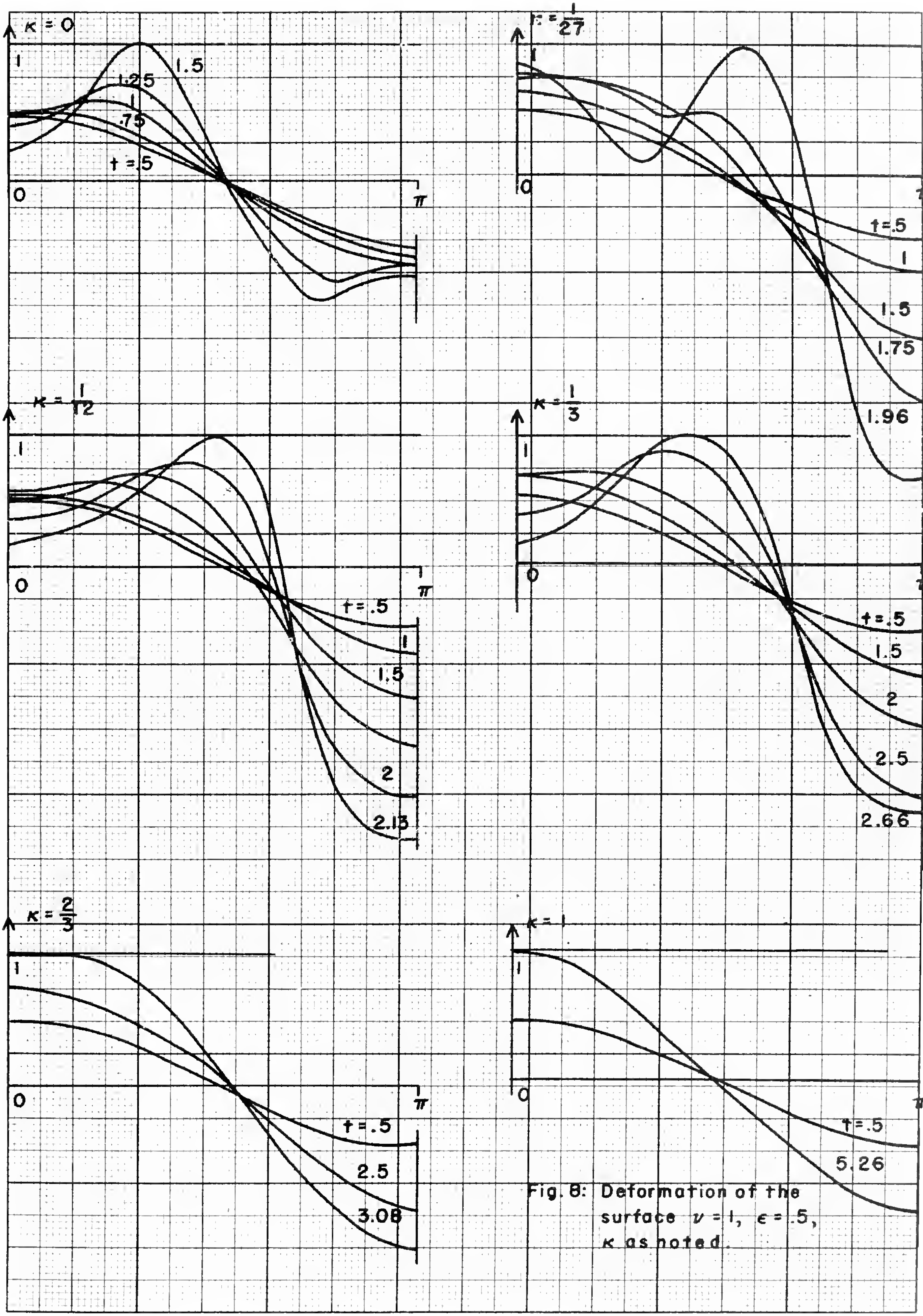

Fig. 8: Deformation of the surface $\nu = 1$, $\epsilon = .5$, κ as noted.

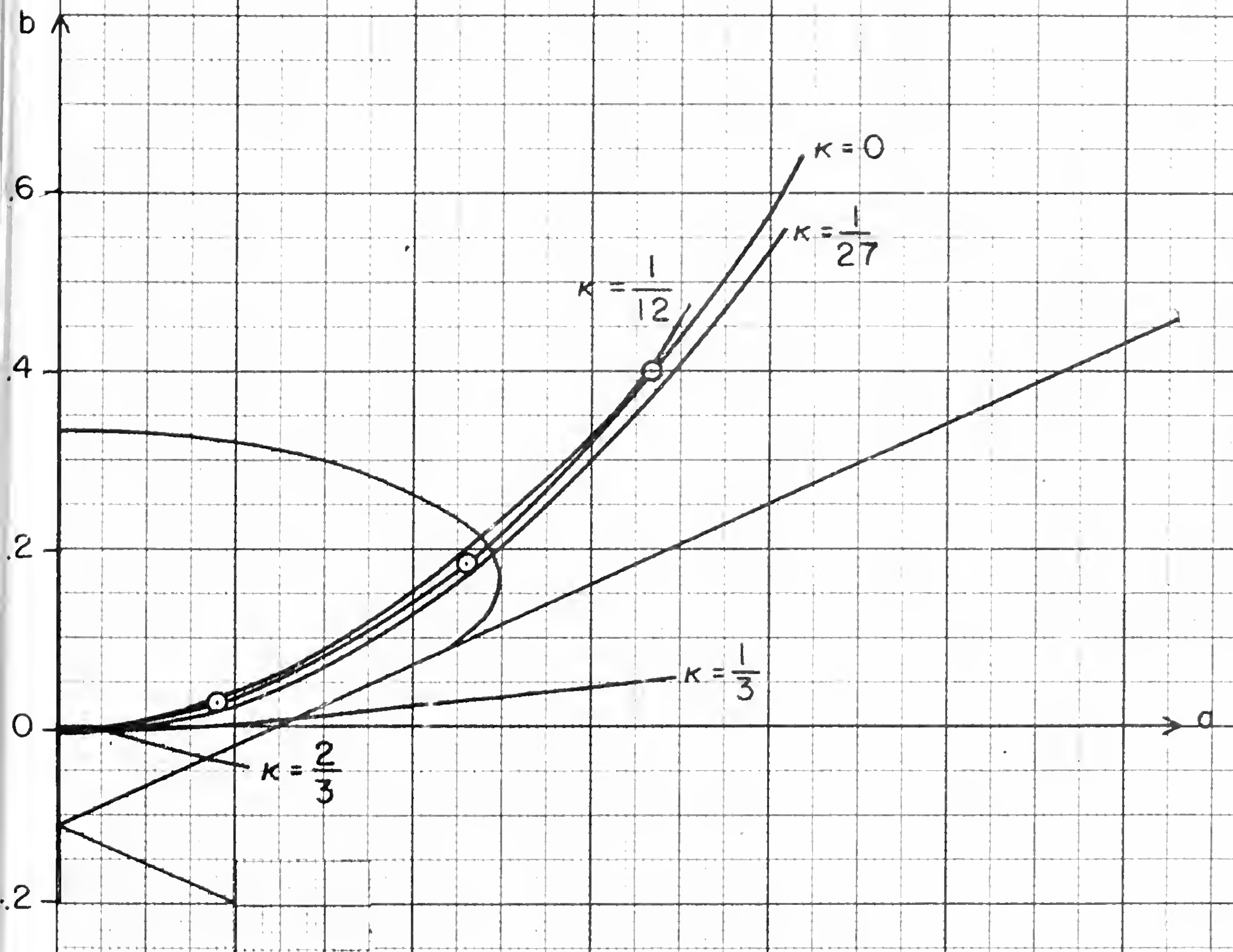

Fig. 9. (a–b) plane diagram for the case $\nu = .2$, $\epsilon = .1$

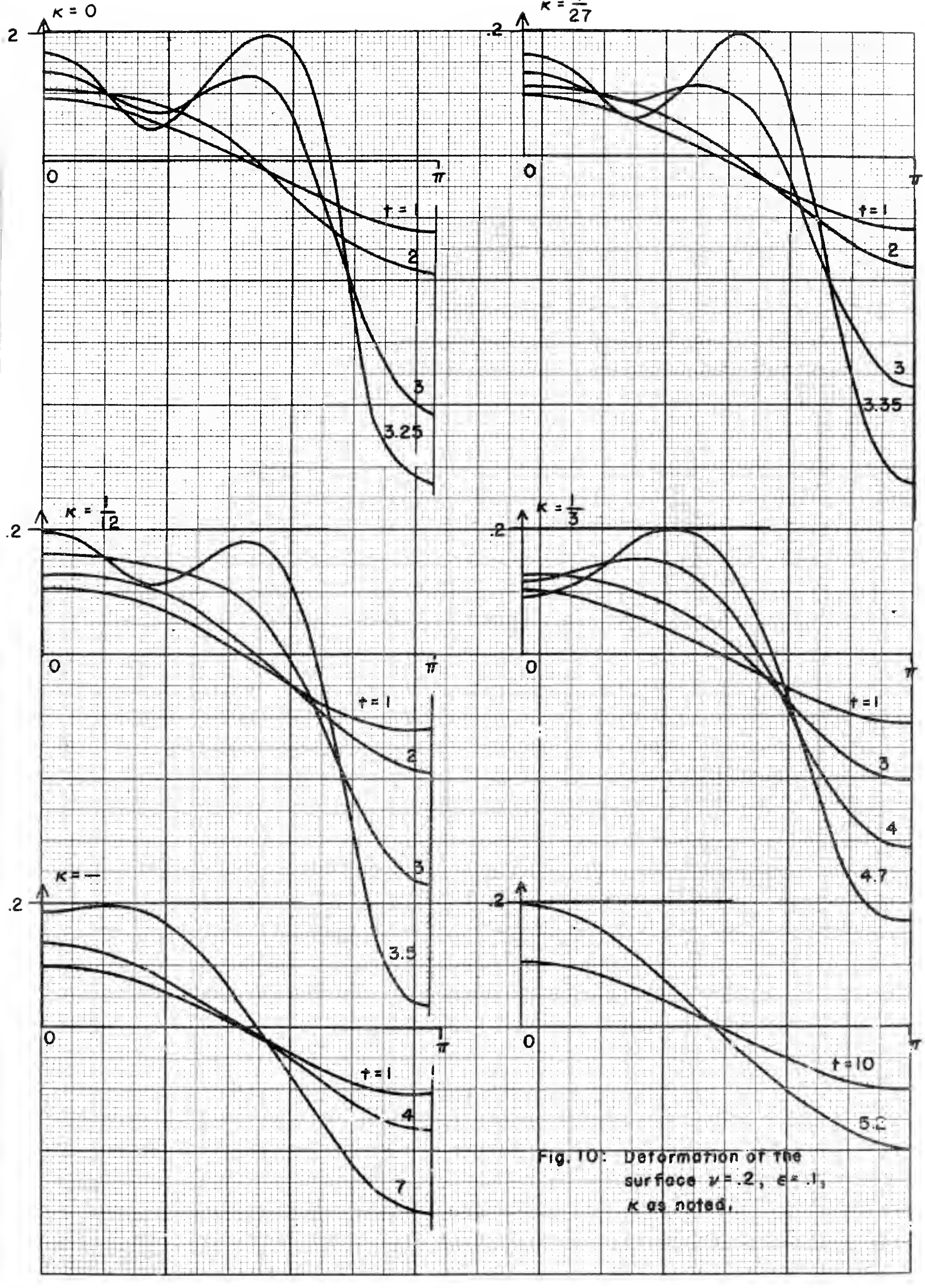

Fig. 10: Deformation of the surface $\nu = .2$, $\epsilon = .1$, κ as noted.

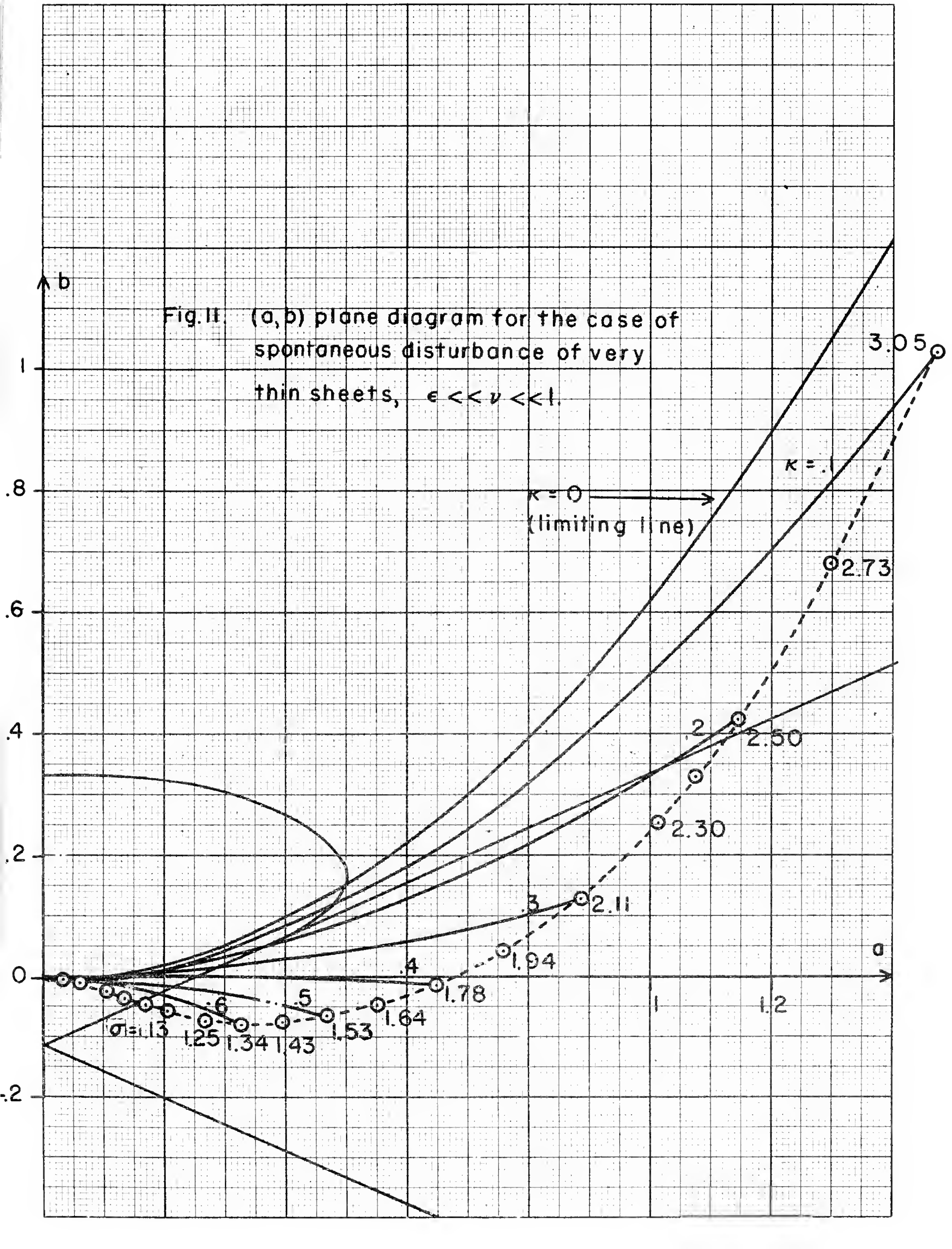

Fig. 11. (a, b) plane diagram for the case of spontaneous disturbance of very thin sheets, $\epsilon << \nu << 1$.

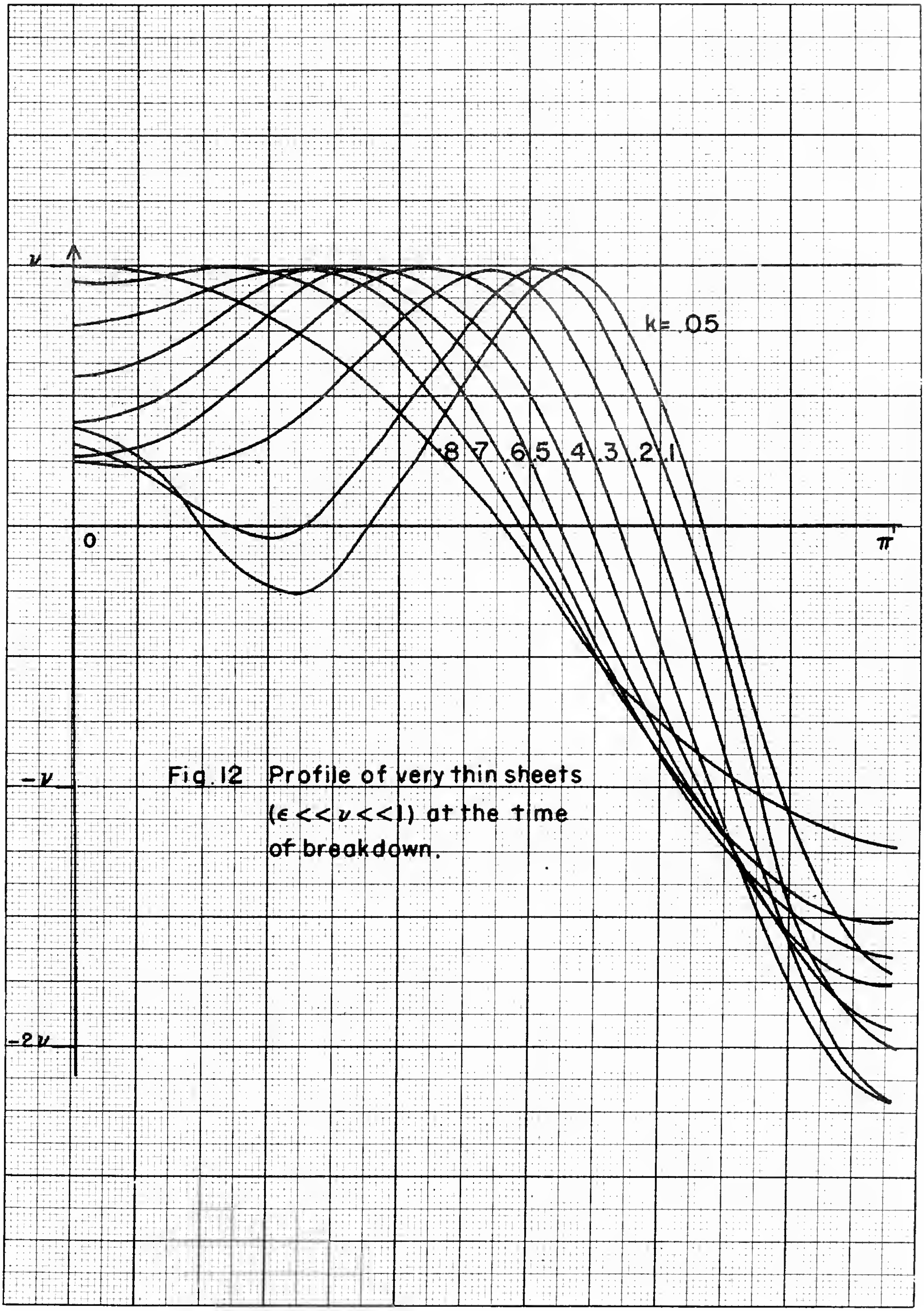

Fig. 12 Profile of very thin sheets ($\epsilon << \nu << 1$) at the time of breakdown.

References.

[1] Bellman R. and Pennington R.H.: "Effects of Surface Tension and Viscosity on Taylor Instability." Princeton University. Report No. PNJ -LA-1 (1952).

[2] Keller J,B. and Kolodner I. I.: "Instability of Liquid Surfaces and the Formation of Drops". J. Appl. Phys. 25 (1954), p 918-921.

[3] Keller J.B. and Kolodner I.I.:"Underwater Explosion Bubbles II. Effects of Gravity and the Change of Shape.". IMS-NYU Report No. 197 (1953).

[4] Layzer D.: "On the Development of Taylor Instability." Princeton University Report No. PNJ-LA-3(1952).

[5] Lewis D.J., Proc. Roy. Soc., A202 (1950) p. 81.

[6] Pennington R. and others: "Machine Calculation of the Growth of Taylor Instability in an Incompressible Fluid." Princeton University Report No. PNJ-LA-11 (1953).

[7] Taylor G., Proc. Roy. Soc. A201 (1950) p. 192.

NYU
IMM
231
Kolodner
Instability of liquid surfaces
and the..